

Cytochrome P450 (CYP) dependent metabolism in HepaRG cells cultured in a dynamic three-dimensional (3D) bioreactor

Malin Damell, Thomas Schreiter, Katrin Zeilinger, Thomas Urbaniak, Therese Söderdahl,
Ingrid Rossberg, Birgitta Dillnér, Anna-Lena Berg, Jörg C. Gerlach, Tommy B. Andersson

DMPK Centre of excellence, AstraZeneca R&D, Mölndal, Sweden (M.D., T.B.A.); Div. of
Experimental Surgery, BCRT, Charité Universitätsmedizin Berlin, Germany (T.S., K.Z., T.U.,
I.R.); Global Safety Assessment, AstraZeneca R&D, Sweden (T.S., B.D., A.L.B); McGowan
Institute for Regenerative Medicine, University of Pittsburgh, PA, USA (J.C.G.); Department
of Physiology and Pharmacology, Karolinska Institutet, Stockholm, Sweden (M.D., T.B.A.).

DMD # 37721

Running title: CYP metabolism studies in bioreactor cultured HepaRG cells

Address for correspondence

Tommy B. Andersson, DMPK Centre of excellence,
AstraZeneca R&D Mölndal, S-431 83 Mölndal, Sweden.
E-mail: tommy.b.andersson@astrazeneca.com

Telephone: +46-31-7761534

Fax: +46-31-7763786

Number of text pages: 16

Number of tables: 2

Number of figures: 8

Word count for abstract: 233 (250 max)

Word count for introduction: 524 (750 max)

Number of words in the discussion: 1330 (1500 max)

Number of references: 33 (40 max)

Abbreviations:

2D, two-dimensional; 3D, three-dimensional; AST, Aspartate aminotransferase; ABC, ATP-binding cassette; CK19, cytokeratin 19; CYP, cytochrome P450; DMSO, dimethyl sulfoxide; IHC, immunohistochemical staining; LDH, lactate dehydrogenase; MDR, multidrug resistance; MRP, multidrug resistance-associated protein; PCR, pFolymerase chain reaction; P-gp, P-glycoprotein.

Abstract

Reliable and stable *in vitro* cellular systems maintaining specific liver functions important for drug metabolism and disposition are urgently needed in preclinical drug discovery and development research. The cell line HepaRG exhibits promising properties such as expression and function of drug metabolizing enzymes and transporter proteins, which resemble those found in freshly isolated human hepatocytes. In this study, HepaRG cells were cultured up to 68 days in a three-dimensional (3D) multi-compartment capillary membrane bioreactor, which enables high-density cell culture under dynamic conditions. The activity of drug metabolizing cytochrome P450 (CYP) enzymes was investigated by a cocktail of substrates for CYP1A1/2 (phenacetin), CYP2C9 (diclofenac), CYP2B6 (bupropion) and CYP3A4 (midazolam). The model CYP substrates, which were introduced to the bioreactor system mimicking *in vivo* bolus doses, showed stable metabolism over the whole experimental period of several weeks with the exception of bupropion hydroxylase, which increased over time. Ketoconazole treatment decreased the CYP3A4 activity by 69% and rifampicin induced the CYP3A4 and CYP2B6 dependent activity 6-fold, which predicts well the magnitude of changes observed *in vivo*. Moreover, polarity of transporter expression and formation of tissue like structures including bile canaliculi was demonstrated by immune histochemistry. The long lasting bioreactor system using HepaRG cells thus provides a promising and stable liver like *in vitro* model for continuous investigations of the hepatic kinetics of drugs and of drug-drug interactions, which well predict the situation *in vivo* in humans.

Introduction

Drug metabolizing enzymes and drug transporters in the liver play a critical role in the clearance and in drug-drug interactions of many medicinal products. Freshly isolated human hepatocytes represent a good model of the liver since they are able to perform the full range of known *in vivo* drug biotransformation pathways and retain many of the uptake and efflux functions of the liver cells (De Bartolo et al., 2006).

However, the use of primary human hepatocytes has several drawbacks such as scarce and unpredictable availability, huge variation in cell functions, especially cytochrome P450 (CYP) activities, as well as a variable response to CYP inducers (Luo et al., 2002; Madan et al., 2003; Abadie-Viollon et al., 2010). The large variation in cell functions can partly be explained by inter-donor variability. However, the variable loss of liver specific functions during cell preparation and in standard *in vitro* culture conditions over time may cause additional variation of hepatocyte performance not related to the normal inter-individual differences found in a population (Rodríguez-Antona et al., 2002).

In vivo, the liver cells are located in a perfused organ where they are arranged in 3D structures forming cell-cell contacts, which are important for the intracellular function and also for maintaining their specific polarity. It has been shown that porcine or human liver cells retain *in vivo* like properties and are arranged in tissue-like structures including formation of biliary canalicular networks and neo-sinusoids when cultured in a perfused three-dimensional (3D) bioreactor (Zeilinger et al., 2004; Schmelzer et al., 2009). Importantly, liver specific functions such as urea and albumin synthesis, glucose metabolism and CYP activities were all maintained for at least 14 days in this type of bioreactor. The multi-compartment bioreactor technology initially described by Gerlach et al. (1994) was developed as a large scale 800 mL clinical bio-artificial liver support system. The technology is based on the use of interwoven hollow fibre capillary membranes that provide independent, decentralized medium and gas

supply to the cells located between the capillaries (Fig. 1). In this study an analytical scale bioreactor with a cell compartment volume of 2 mL was used for drug metabolism studies.

HepaRG cells are an attractive alternative to primary human hepatocytes since they exhibit important functions for drug metabolism and disposition such as CYP-, UDP-glucuronosyltransferase (UGT) and transporter activities (Aninat et al., 2006; Le Vee et al., 2006; Hart et al., 2010; Kanebratt and Andersson, 2008a). Recently, HepaRG cells in 2D cultures were evaluated as a valuable *in vitro* model for prediction of CYP induction *in vivo* in humans (Kanebratt and Andersson, 2008b).

In the present study HepaRG cells cultured in the analytical scale 3D bioreactor system were used to study the function of four major drug metabolizing enzymes, CYP1A1/2, CYP2C9, CYP2B6 and CYP3A4. Especially the long-term stability of CYP enzyme expression and function was assessed by repeating CYP activity studies over several weeks. Furthermore, the ability to induce and inhibit CYP activities by the well-characterized model inducer rifampicin and the inhibitor ketoconazole was sequentially investigated in the same bioreactor culture. The results were also compared with published *in vivo* results to evaluate the predictive value of the observed effects.

Materials and Methods

Bioreactor technology

The bioreactor technology is based on three independent interwoven capillary systems integrated into a polyurethane housing (Fig. 1). Two of the capillary systems serve for counter-current medium perfusion and a third set of capillaries serves for direct, decentralized gas exchange via diffusion. The cells reside in the cell compartment between the capillaries, which form a three-dimensional scaffold. A port enables substance injection, mimicking bolus administration, and sampling from the re-circulating medium. Fresh medium is continuously supplied from the medium bottle and excess medium flows out into the outflow bottle (Fig. 1c). A detailed description of the bioreactor structure is given elsewhere (Schmelzer et al., 2009). In this study, a down-scaled bioreactor with a cell compartment volume of 2 ml was used (Fig. 1b).

Proliferation and differentiation of HepaRG cells

The cells were first proliferated in 2D flasks prior to bioreactor inoculation. The enriched HepaRG medium (Biopredic International, Rennes, France) composed of Williams' medium E with GlutaMAX-I, supplemented with 10% fetal bovine serum, 100 IU/ml penicillin, 100 µg/ml streptomycin, 5 µg/ml bovine insulin and 50 µM hydrocortisone hemisuccinate was changed 5 times in two weeks during 2D culture. The cells were trypsinated and 83 ± 40 millions of cells were inoculated into the cell compartment of the bioreactor (n=3). The cells had a viability above 90% as determined by Trypan blue staining. The proliferation phase was continued in the bioreactor for one to two weeks using enriched HepaRG medium (Biopredic International, Rennes, France). The differentiation of the cells was induced by changing the re-circulating medium to high DMSO HepaRG medium (Biopredic International, Rennes, France) composed of enriched medium with addition of 2% DMSO. The cells were allowed to differentiate for two weeks, then the high DMSO medium was washed out and changed back

to enriched HepaRG medium (Fig. 2). Since the cells were both expanded and differentiated in the bioreactor an initial long lead time was needed before the first experiments could be performed. However, we are currently designing a bioreactor model where fully differentiated cryopreserved HepaRG cells are inoculated into the bioreactor, which will significantly shorten the lead time.

Immunostaining

Samples from cell culture material were taken from different locations within the bioreactor capillary network upon culture termination. After fixation in 5% paraformaldehyde the material was dehydrated, embedded in paraffin and cut into approximately 5 μm -sections. The immunohistochemical staining (IHC) was performed on the staining module Discovery XT (Ventana® Medical Systems Inc, Tucson, USA). Antibodies in use were MDR1 (P-gp, clone F4, Sigma-aldrich, Saint Louis, USA), MRP2 (clone M2 III-6, Abcam, Cambridge, UK) and CYP3A4 (Cypex, Scotland, UK). All solutions for deparaffinization, pretreatment, detection, counterstaining and rinsing steps, were supplied by Ventana® Medical systems Inc. Heat (20 min for MDR1 in a citrate buffer pH 6 or 40 min for MRP2 in a Tris/borate/EDTA buffer, pH 8, at 98°C) or enzyme (protease 8 min at 37 °C, for CYP3A4) were used as antigen retrieval pretreatment. Both primary and secondary antibodies were diluted in Discovery Ab Diluent. The IHC was visualized with diaminobenzidine chromogen (DAB) and the counterstaining was performed with haematoxylin.

For immunofluorescence (IF) staining of cytokeratin 19 (CK19), sections were deparaffinized with xylene and rehydrated with a series of decreasing concentrations of alcohol. Antigens were retrieved by boiling sections for 25 min in citrate buffer (0.01 citric acid monohydrate, pH 6.0; Merck, Darmstadt, Germany) followed by incubation for 20 min in 5% Triton/PBS. Sections were blocked with 5% skimmed milk, followed by incubation with monoclonal mouse anti-CK19 IgG1 (Santa Cruz Biotechnology, Santa Cruz, USA) for 30

min. Cy2-conjugated polyclonal goat anti-mouse IgG (Dianova, Hamburg, Germany) was used as secondary antibodies. For non-specific staining of the nuclei, sections were incubated with 4',6-diamidino-2-phenylindole (DAPI, Molecular Probes, Leiden, Germany).

Subsequently the sections were mounted with Aqua Polymount solution (Polysciences Inc., Warrington, PA, USA).

Determination of clinical chemistry parameters

Biochemical parameters related to the cell integrity and to the synthesis capability of HepaRG cells were measured daily in samples from the culture perfusate and/or the medium outflow. Concentrations of lactate were determined by means of an automated cell culture analyzer (Bioprofile analyzer 100plus, IUL instruments GmbH, Königswinter, Germany). Activities of lactate dehydrogenase (LDH) and aspartate aminotransferase (AST) were measured with an automated clinical chemistry analyser (Modular P800, Roche Diagnostics, Mannheim, Germany) using the corresponding assay kits from Roche/ Cobas). Human albumin was quantified using ready-to-use ELISA test kits (Exocell, Philadelphia, PA, USA).

The daily production of biochemical parameters in the bioreactors was calculated on the basis of concentrations measured in the outflow bottle and in the perfusion circuit (Fig. 1), according to the following formula:

$$P / \Delta t = (C_O - C_M) * V_O / \Delta t + (C_d - C_{d-1}) * V_R / \Delta t$$

P = Total production rate, Δt = time interval between two sampling time points, C_O = concentration in the outlet vessel, C_M = medium blank concentration, V_O = volume of medium in the outlet vessel, C_d = concentration in perfusate at the time point of sample taking, C_{d-1} = concentration in the previously taken sample from the perfusate, V_R = recirculating volume.

The average daily production was calculated for the proliferation phase (8-14 days), the differentiation phase (14 days) and the experimental phase (26-37 days) by dividing the total production during the whole phase by the number of days the phase lasted. Subsequently, the

mean values and standard derivations were calculated for the three bioreactors. The parameters are presented as mg/day/bioreactor or Unit/day/bioreactor.

CYP activity measurements

CYP activity was assessed by adding a CYP cocktail through the sampling port close to the bubble trap (Fig. 1c). The medium in the bubble trap was mixed a few times before starting the recirculation of the medium ($t = 0$ h), allowing the substrate to reach the cells in the bioreactor. The CYP cocktail consisted of phenacetin (CYP1A1/2), midazolam (CYP3A4), diclofenac (CYP2C9) and bupropion (CYP2B6). The metabolites were measured in the medium over a period of 6 h. The parent drugs phenacetin and diclofenac (both from Sigma-Aldrich, Deisenhofen, Germany) were prepared as 20 mmol/L stock solutions in DMSO and diluted in culture medium to achieve final concentrations of 26 $\mu\text{mol/L}$ and 9 $\mu\text{mol/L}$, in the bioreactor circuit. Midazolam was provided as an aqueous solution (Dormicum®, Roche Pharma, Grenzach-Wyhlen, Germany) at 13.8 mmol/L (5mg/ml) and diluted to a final concentration of 3 $\mu\text{mol/L}$. Bupropion (Toronto Research Chemicals Inc, Canada) was prepared as a 50 mmol/L aqueous stock solution and diluted to a final concentration of 100 $\mu\text{mol/L}$.

Analysis of the CYP metabolism was performed at continuous medium perfusion, but without feeding medium into the perfusion circuit (closed-system perfusion). Samples (200 μl) were taken at 0, 0.25, 0.5, 1, 2, 4 and 6 h. After each experiment the bioreactor circuit was rinsed with 75 ml of culture medium (single-pass perfusion) and was then reset to the standard operation mode with continuous medium feed (open-system perfusion). Samples were frozen until further processing. The activities were measured as an increase in metabolite concentration in the medium. No attempts were made to relate the activities to the total amount of protein or number of cells, since this is difficult to assess in the bioreactor. However, the effects on CYP activities by ketoconazole and rifampicin are presented as

relative changes in the bioreactors containing differentiated cells, thus the absolute amount of proteins or cells are not important for interpretation of the results.

CYP activity experiments

The experiments were conducted in differentiated HepaRG cells 3 days after DMSO removal, which was the time for the first basal CYP activity measurement (CYP activity 1, Fig. 2). The effects of ketoconazole and rifampicin on CYP activities were compared with activities measured directly before introducing the interacting compound in a time course of experiment as depicted in Fig. 2. CYP activity 2 is thus used to calculate the effect of ketoconazole (CYP activity 3) and CYP activity 4 is the basal activity used to compare with the activity in rifampicin treated cells (CYP activity 5). CYP activity 6 is the last experiment determining the basal activity before samples were removed for immunohistochemical staining.

Ketoconazole (3 μ M final concentration) was introduced 0.5 h prior to addition of the CYP cocktail to the recirculating medium. To measure the effect of rifampicin the cells were exposed to 20 μ M (final concentration) rifampicin for 60 h. Rifampicin was washed out from the bioreactor circuit for 12 h, before CYP activities were measured in order to avoid direct interaction of rifampicin with the CYP substrates. The experimental phase lasted for two to four weeks (n=3).

Analysis of marker substrates and metabolites

1'-hydroxymidazolam, paracetamol, 4'-hydroxydiclofenac and hydroxybupropion were analysed using liquid chromatography/mass spectrometry. The liquid chromatography system consisted of a HTS PAL injector (CTC Analytics, Zwingen, Switzerland) combined with an HP 1100 LC binary pump and column oven (Agilent Technologies Deutschland, Waldbronn, Germany). The separation was performed on a reversed-phase HyPurity C18 analytical column (50 \times 2.1 mm, 5 μ m, Thermo, UK) with a HyPurity C18 precolumn at 40 $^{\circ}$ C

and with a flow rate of 750 $\mu\text{l}/\text{min}$. The mobile phases consisted of 0.1% (v/v) formic acid in 5% acetonitrile (A) and 0.1% (v/v) formic acid in 95% acetonitrile (B). The organic modifier content B was increased linearly from 2 to 40 % over 2 min and from 40 to 98% over 1.4 min. Then it was maintained at 98 % for 0.5 min and decreased to 2 % in 0.1 min. Detection was performed with a triple quadrupole mass spectrometer, API4000, equipped with an electrospray interface (Applied Biosystems/MDS Sciex, Concord, Canada). The mass spectrometry parameters were optimized using each analyte. The compound dependent parameters were as follows: the collision energy was set at 45 V, 20 V, 20 V and -15 V for 1'-hydroxymidazolam, paracetamol, hydroxybupropion and 4'-hydroxydiclofenac, respectively. The collision activated dissociated gas was 10 for 1'-hydroxymidazolam, paracetamol and hydroxybupropion and 7 for 4'-hydroxydiclofenac. The transition chosen were 256.1 > 238 for hydroxybupropion, 309.9 > 265.8 for 4'-hydroxydiclofenac, 342.1 > 203.0 for 1'-hydroxymidazolam and 152.1 > 109.9 for paracetamol. A dwell time of 100 ms was used and the limit of quantification was 5 nmol/L. Instrument control, data acquisition and data evaluation were performed using Applied Biosystems/MDS Sciex Analyst 1.4 software.

Calculations

Linear regression was used to describe data for 4'-hydroxydiclofenac, 1'-hydroxymidazolam, paracetamol and hydroxybupropion (Fig. 6-8) using GraphPad Prisma 4.0.3 (GraphPad Software, Inc, La Jolla, California, USA). The data for 1'-hydroxymidazolam after rifampicin treatment were described by nonlinear regression using a polynomial second order equation (Fig 8).

Formation rates of the metabolites were calculated over the 6 h experiment for paracetamol, 1'-hydroxymidazolam, 4'-hydroxydiclofenac and hydroxybupropion using the slope of the amount (nmol) vs. time (h) graph. Only the 2 first hours of the experiment were used to calculate the formation rate of 1'-hydroxymidazolam after rifampicin treatment

DMD # 37721

(GraphPad Prisma 4.0.3). The change in enzyme activities by rifampicin treatment was calculated by dividing formation rate values after rifampicin treatment by the corresponding values before rifampicin treatment.

Statistical Analysis

The possible significance of the effect of rifampicin or ketoconazole on the formation rate values of 1'-hydroxymidazolam or hydroxybupropion was calculated using the two-tailed student t-test. The same test was used to calculate the significance of differences between the first and last CYP activity experiment.

Results

Immunostaining of CYP3A4, P-gp, MRP2 and CK19

Cell material was removed from the bioreactor cell compartment after the CYP activity measurements and used for staining of P-gp (ABCB1), MRP2 (ABCC2), CYP3A4 and cytokeratin 19 (CK19) by monoclonal antibodies. Histological pictures showed the formation of tissue-like cell aggregates between the capillaries (figure 3). As indicated in figure 3 (a, b and c), CYP3A4 and the apical efflux transporters P-gp and MRP2 were all present in the bioreactor tissue. CYP3A4 was found to be expressed in the hepatocyte-like cells and both P-gp and MRP2 were located to one side of the hepatocyte-like cells forming bile canaliculi-like structures. The biliary marker CK19 was detected in strand-like structures within the cell aggregates as shown in figure 4.

Clinical chemistry parameters

Clinical chemistry analyses of the medium perfusate were performed daily during the culture period. The mean values (n=3) of the daily medium values are shown for the proliferation, differentiation and experimental phases in figure 5. Lactate production significantly ($p < 0.01$) decreased by 34% during the differentiation phase compared to the proliferation phase, whereas no significant change was observed in albumin production (Fig. 5 a). The lactate and albumin production in the bioreactor inoculated with HepaRG cells was comparable to what has been observed in bioreactors inoculated with human hepatocytes (Zeilinger et al., 2011). The release of LDH and AST was low and stable over the whole culture period (Fig. 5 b).

Basal levels and the effect of ketoconazole and rifampicin on CYP activities

The CYP2C9, CYP1A1/2 or CYP3A4 mediated activities, calculated as the formation rates of the metabolites over the 6 h experiment, showed no difference between the first (CYP

activity 1 in Fig. 2) and the last (CYP activity 6 in Fig. 2) CYP experiment (Fig. 6 a, b, c). However, the rate of CYP2B6 dependent hydroxybupropion formation increased 3.6-fold between the first and last experiment (Fig. 6 d).

Ketoconazole and rifampicin were introduced into the bioreactor as depicted in Figure 2. The effects of ketoconazole and rifampicin on CYP activities were compared with the activities measured directly before introducing the interacting compounds. Ketoconazole was introduced into the system and the direct effects on the CYP mediated activities were investigated. The 1'-hydroxymidazolam formation rate decreased by 69% ($p < 0.05$, Table 1, Fig. 7) upon ketoconazole treatment, whereas the CYP2C9, CYP2B6 and CYP1A1/A2 dependent activities were not affected (data not shown).

The cell culture was exposed to rifampicin for 60 h and then washed out for 12 h before investigating CYP activities to avoid direct interaction of rifampicin with enzyme activity measurements. The CYP3A4 dependent 1'-hydroxymidazolam formation increased 6-fold upon rifampicin treatment ($p \leq 0.05$) (Table 2 a, Fig 8 a). Further, CYP2B6 dependent bupropion hydroxylase activity was 6-fold higher after rifampicin treatment ($p < 0.01$, Table 2 b, Fig. 8 b), whereas phenacetin O-dealkylase (CYP1A1/2) and diclofenac 4'-hydroxylase (CYP2C9) activities were unaffected by rifampicin (data not shown).

Discussion

HepaRG cells represent a highly differentiated cell line, which exhibits several important human liver functions such as drug metabolism and drug transporter activities (Aninat et al., 2006; Le Vee et al., 2006). In the present study, HepaRG cells were cultured in a dynamic 3D bioreactor system to evaluate the suitability of this experimental set up as a human hepatic *in vitro* model for drug metabolism and disposition studies.

Confluent HepaRG cells are known to differentiate into both hepatocyte-like and biliary-epithelial-like cells (Aninat et al., 2006; Guillouzo et al., 2007). Both cell types were present in the bioreactor and the proportion between the two cell types were presumed to remain constant in the differentiated state when experiments were performed. The relative effects on CYP activities caused by ketoconazole and rifampicin that was evaluated in this study could thus reliably be calculated and compared with effects reported in other *in vitro* and *in vivo* studies. The hepatocyte-like cells were polarized as revealed by immunostaining of the transporter proteins P-gp and MRP2, which were located at one side of the cell. The P-gp and MRP2 positive sides of the cells were also facing each other, which resembles the situation *in vivo* where these transporters are located at the apical membranes of hepatocytes forming bile canaliculi-like structures. Strand-like formations of CK19 positive cells indicate the formation of biliary structures. Thus, the HepaRG cells in the bioreactor seem to develop structures that resemble liver tissue *in vivo*. Studies are ongoing to characterize in more detail the biliary structures and the function of transporters in the bioreactor.

The stable albumin production observed over the whole culture period further implies a liver like function of HepaRG cells when cultured in the bioreactor. Lactate production decreased significantly during differentiation, which can be explained by decreasing glucose metabolism due to a decrease in proliferation associated with ongoing differentiation. Further, the albumin and lactate production were at the same level as observed for primary human hepatocyte cultured in the same bioreactor prototype (Zeilinger et al., 2011). The stable and

low release of LDH and AST from cells indicates that no significant cell damage occurred during bioreactor cultivation.

CYP1A1/2, CYP2C9 and CYP3A4 mediated activities were stable for several weeks in the bioreactor culture of differentiated cells, which is important for the performance of long-term studies on drug metabolism. CYP2B6 even showed an increased activity over time in the bioreactor. The reason for this observation should be studied further.

It is known that nonspecific binding of substances to material in different types of bioreactor systems (including conventional 2D systems) can be a problem (Toepke and Beebe, 2006; Chao et al., 2009). The nonspecific binding properties of the substances used in the present study were not investigated. However, the initial metabolite formation was linear, thus the substrate concentrations are not likely to be rate limiting for enzyme activities. In addition, the magnitude of induction by rifampicin and inhibition by ketoconazole seen in this study were comparable with HepaRG and hepatocytes cultured in 2D and with *in vivo* studies as discussed below indicating sufficient access to the substrates used.

Inhibition of CYP enzymes is the most common cause of drug-drug interactions *in vivo*. In this study, ketoconazole was used, which is a commonly used and well characterized strong CYP3A inhibitor in humans both *in vitro* and *in vivo* (Turpeinen et al., 2009). Midazolam is a sensitive CYP3A probe for CYP3A activity *in vivo*. In humans, the clearance of midazolam has been reported to be reduced by about 85% by ketoconazole (Tsunoda et al., 1999; Tham et al., 2006; Yong et al., 2008; Krishna et al., 2009), which is comparable with the 69% decrease in the formation rate of 1'-hydroxymidazolam seen in the bioreactor in this study using HepaRG cells. A comparable degree of inhibition (83 to 100%) of the 1'-hydroxymidazolam formation rate by 10 μ M ketoconazole has also been reported in 2D cultured primary human hepatocytes from 18 donors (Klieber et al., 2008). CYP2C9 dependent inhibition by ketoconazole was not recorded in this experiment. However it has been shown that the potency by which CYP2C9 is inhibited by ketoconazole is about 10-fold

lower than for CYP3A4 (Kumar et al., 2006). The ketoconazole concentration may thus be too low to significantly inhibit CYP2C9 dependent diclofenac hydroxylation in the bioreactor.

Induction of CYP3A *in vivo* is often measured as an increase in midazolam clearance. When midazolam was administered intravenously, the average induction of midazolam clearance by rifampicin was reported to be 2-fold (Floyd et al., 2003; Gorski et al., 2004; Yu et al., 2004; Kharasch et al., 2004). In the study by Gorski et al. (2004) the range of induction of midazolam clearance by rifampicin was reported to be between 1.4- and 7.4 –fold. In this study, the rifampicin induction of CYP3A4 activity was 6 ± 4 -fold, when measured as the formation rate of 1'-hydroxymidazolam. The fold induction in HepaRG cells cultured in the bioreactor is thus in the same range as seen *in vivo* and also close to the 8 ± 3 -fold induction seen for CYP3A4 activity by rifampicin in 2D plated HepaRG cells (Kanebratt and Andersson, 2008b). In primary human hepatocytes the effect of rifampicin on CYP3A4 can vary considerably. Abadie-Viollon et al. (2010) reported a range of induction by rifampicin between 2- to 19-fold in hepatocytes from 21 donors. The range of CYP3A induction responses in primary human hepatocytes from different subjects by rifampicin is thus larger than the variation reported *in vivo* measured as midazolam clearance. The larger variation in induction response observed in human hepatocytes may be caused by the erratic loss of liver specific functions in culture of human hepatocytes resulting in low basal levels of CYP3A4 enzymes before exposing the cells to potential inducers (Luo et al., 2002). However, the induction response of CYP3A activity by rifampicin measured in microsomes prepared from sandwich cultured human hepatocytes from six different donors was close to the range seen *in vivo* (Luo et al., 2002; Gorski et al., 2004).

The 6 ± 2 -fold increase (n=3) in hydroxybupropion formation rates by rifampicin pre-treatment in the bioreactor is consistent with the 3- to 5-fold increase (n=10) in hydroxybupropion formation rates observed in humans *in vivo* (Kharasch et al., 2008) as well as with the 3- to 3.4-fold increased (n=16) clearance of bupropion *in vivo* (Loboz et al., 2006).

This is also comparable with the 6 ± 2 -fold CYP2B6 activity increase in 2D cultured HepaRG cells (Kanebratt and Andersson, 2008b). In cultured primary human hepatocytes, however, a large variation in induction of bupropion hydroxylase activity by rifampicin has been reported. Abadie-Viollon et al. (2010) described a 0- to 21- fold induction by rifampicin using cells from 22 donors. Thus, the magnitude of induction *in vivo* seems to be better reflected by HepaRG cells compared to primary human hepatocytes.

CYP2C9 was not significantly induced by rifampicin in this study. CYP2C9 is known to show a weaker induction response *in vivo* to rifampicin treatment than CYP3A (Kanebratt et al., 2008c). A considerable weaker induction response of CYP2C9 as compared to CYP3A4 by rifampicin has also been reported in studies in cryopreserved human hepatocytes (Fahmi et al., 2010).

In conclusion, the bioreactor using HepaRG cells showed stable functions over several weeks allowing the performance of long-term sequential studies using the same cell culture system. HepaRG cells aggregated in the bioreactor and formed tissue like structures including bile canaliculi. Polarity of transporter protein expression similar to those seen *in vivo* was observed, which opens up for the development of an *in vivo* like liver model. The CYP activities were in general stable over the whole experimental period and the effects of rifampicin and ketoconazole on CYP activities in the bioreactor predict well the effects observed *in vivo*. These findings using HepaRG cells in the bioreactor are promising and the model could potentially be developed into a long-lasting liver like model for investigations of the contribution of the liver to the kinetics of drugs *in vivo* and for predictive studies of drug-drug interactions in humans.

Acknowledgements

We thank Wolfgang Mudra for graphical illustration.

DMD # 37721

Authorship Contributions

Participated in research design: Andersson, Darnell, Schreiter, Zeilinger, Gerlach and Berg

Contributed with new research tools: Gerlach

Conducted experiments: Schreiter, Darnell, Urbaniak, Dillnér and Söderdahl

Performed data analysis: Darnell, Schreiter, Urbaniak, Rossberg, Dillnér and Berg

Wrote or contributed to the writing of the manuscript: Andersson, Darnell, Zeilinger,

Schreiter, Dillner and Urbaniak

References

- Abadie-Viollon C, Martin H, Blanchard N, Pekthong D, Bachellier P, Manton G, Heyd B, Schuler F, Coassolo P, Alexandre E, Richert L. (2010) Follow-up to the pre-validation of a harmonised protocol for assessment of CYP induction responses in freshly isolated and cryopreserved human hepatocytes with respect to culture format, treatment, positive reference inducers and incubation conditions. *Toxicology in Vitro* **24**:346-356.
- Aninat C, Piton A, Glaise D, Le Charpentier T, Langouet S, Morel F, Guguen-Guillouzo C, Guillouzo A. (2006) Expression of cytochromes P450, conjugating enzymes and nuclear receptors in human hepatoma HepaRG cells. *Drug Metab Dispos* **34**:75-83.
- Chao P, Maguire T, Novik E, Cheng K-, and Yarmush ML. (2009) Evaluation of a microfluidic based cell culture platform with primary human hepatocytes for the prediction of hepatic clearance in human. *Biochem Pharmacol* **78**:625-632.
- De Bartolo L, Salerno S, Morelli S, Giorno L, Rende M, Memoli B, Procino A, Andreucci VE, Bader A, Drioli E. (2006) Long-term maintenance of human hepatocytes in oxygen-permeable membrane bioreactor. *Biomaterials* **27**:4794-4803.
- Fahmi OA, Kish M, Boldt S, and Obach RS. (2010) Cytochrome P450 3A4 mRNA is a more reliable marker than CYP3A4 activity for detecting pregnane X receptor-activated induction of drug-metabolizing enzymes. *Drug Metab Dispos* **38**:1605-1611.
- Floyd MD, Gervasini G, Masica AL, Mayo G, George AL, Jr, Bhat K, Kim RB, and Wilkinson GR. (2003) Genotype-phenotype associations for common CYP3A4 and CYP3A5 variants in the basal and induced metabolism of midazolam in European- and African-American men and women. *Pharmacogenetics* **13**:595-606.

Gerlach JC, Encke J, Hole O, Muller C, Ryan CJ, Neuhaus P. (1994) Bioreactor for a larger scale hepatocyte in vitro perfusion. *Transplantation* **58**:984-988.

Gorski JC, Huang SM, Pinto A, Hamman MA, Hilligoss JK, Zaheer NA, Desai M, Miller M, and Hall SD. (2004) The effect of echinacea (*Echinacea purpurea* root) on cytochrome P450 activity in vivo. *Clin Pharmacol Ther* **75**:89-100.

Guillouzo A, Corlu A, Aninat C, Glaise D, Morel F, Guguen-Guillouzo C. (2007) The human hepatoma HepaRG cells: A highly differentiated model for studies of liver metabolism and toxicity of xenobiotics. *Chemico-Biological Interactions* **168**:66-73.

Hart SN, Li Y, Nakamoto K, Subileau EA, Steen D, Zhong XB. (2010) A comparison of whole genome gene expression profiles of HepaRG cells and HepG2 cells to primary human hepatocytes and human liver tissues. *Drug Metab Dispos* **38**:988-994.

Kanebratt KP and Andersson TB. (2008a) Evaluation of HepaRG cells as an in vitro model for human drug metabolism studies. *Drug Metab Dispos* **36**:1444-1452.

Kanebratt KP and Andersson TB. (2008b) HepaRG cells as an in vitro model for evaluation of cytochrome P450 induction in humans. *Drug Metab Dispos* **36**:137-45.

Kanebratt KP, Diczfalusy U, Bäckström T, Sparve E, Bredberg E, Böttiger Y, Andersson TB, Bertilsson L. (2008c) Cytochrome P450 induction by rifampicin in healthy subjects: determination by the Karolinksa cocktail and the endogenous marker for 4 β -hydroxycholesterol. *Clin Pharmacol Ther* **84**: 589-594.

Kharasch ED, Walker A, Hoffer C, and Sheffels P. (2004) Intravenous and oral alfentanil as in vivo probes for hepatic and first-pass cytochrome P450 3A activity: noninvasive assessment by use of pupillary miosis. *Clin Pharmacol Ther* **76**:452-466.

Kharasch ED, Mitchell D, Coles R. (2008) Stereoselective bupropion hydroxylation as an in vivo phenotypic probe for cytochrome P4502B6 (CYP2B6) activity. *J Clin Pharmacol* **48**:464-474.

Klieber S, Hugla S, Ngo R, Arabeyre-Fabre C, Meunier V, Sadoun F, Fedeli O, Rival M, Bourrie M, Guillou F, Maurel P, Fabre G. (2008) Contribution of the N-glucuronidation pathway to the overall in vitro metabolic clearance of midazolam in humans. *Drug Metab Dispos* **36**:851-862.

Krishna G, Moton A, Ma L, Savant I, Martinho M, Seiberling M, and McLeod J. (2009) Effects of oral posaconazole on the pharmacokinetic properties of oral and intravenous midazolam: a phase I, randomized, open-label, crossover study in healthy volunteers. *Clin Ther* **31**:286-298.

Kumar V, Wahlstrom JL, Rock DA, Warren CJ, Gorman LA, and Tracy TS. (2006) CYP2C9 inhibition: impact of probe selection and pharmacogenetics on in vitro inhibition profiles. *Drug Metab Dispos* **34**:1966-1975.

Le Vee M, Jigorel E, Glaise D, Gripon P, Guguen-Guillouzo C, Fardel O. (2006) Functional expression of sinusoidal and canalicular hepatic drug transporters in the differentiated human hepatoma HepaRG cell line. *European Journal of Pharmaceutical Sciences* **28**:109-117.

Loboz KK, Gross AS, Williams KM, Liauw WS, Day RO, Blievernicht JK, Zanger UM, and McLachlan AJ. (2006) Cytochrome P450 2B6 activity as measured by bupropion hydroxylation: effect of induction by rifampin and ethnicity. *Clin Pharmacol Ther* **80**:75-84.

Luo G, Cunningham M, Kim S, Burn T, Lin J, Sinz M, Hamilton G, Rizzo C, Jolley S, Gilbert D, Downey A, Mudra D, Graham R, Carroll K, Xie J, Madan A, Parkinson A, Christ D, Selling B, LeCluyse E, Gan LS. (2002) CYP3A4 induction by drugs: Correlation between

a pregnane X receptor reporter gene assay and CYP3A4 expression in human hepatocytes.

Drug Metab Dispos **30**:795-804.

Madan A, Graham RA, Carroll KM, Mudra DR, Burton LA, Krueger LA, Downey AD, Czerwinski M, Forster J, Ribadeneira MD, Gan LS, LeCluyse EL, Zech K, Robertson P, Jr, Koch P, Antonian L, Wagner G, Yu L, and Parkinson A. (2003) Effects of prototypical microsomal enzyme inducers on cytochrome P450 expression in cultured human hepatocytes.

Drug Metab Dispos **31**:421-431.

Rodríguez-Antona C, Donato MT, Boobis A, Edwards RJ, Watts PS, Castell JV, and Gómez-Lechón M-. (2002) Cytochrome P450 expression in human hepatocytes and hepatoma cell lines: Molecular mechanisms that determine lower expression in cultured cells. *Xenobiotica* **32**:505-520.

Schmelzer E, Mutig K, Schrade P, Bachmann S, Gerlach JC, Zeilinger K. (2009) Effect of human patient plasma ex vivo treatment on gene expression and progenitor cell activation of primary human liver cells in multi-compartment 3D perfusion bioreactors for extra-corporeal liver support. *Biotechnol Bioeng* **103**:817-827.

Tham LS, Lee HS, Wang L, Yong WP, Fan L, Ong AB, Sukri N, Soo R, Lee SC, Goh BC. (2006) Ketoconazole renders poor CYP3A phenotype status with midazolam as probe drug. *Ther Drug Monit* **28**:255-261.

Toepke MW and Beebe DJ. (2006) PDMS absorption of small molecules and consequences in microfluidic applications. *Lab Chip* **6**:1484-1486.

Tsunoda SM, Velez RL, von Moltke LL, and Greenblatt DJ. (1999) Differentiation of intestinal and hepatic cytochrome P450 3A activity with use of midazolam as an in vivo probe: effect of ketoconazole. *Clin Pharmacol Ther* **66**:461-471.

Turpeinen M, Tolonen A, Chesne C, Guillouzo A, Uusitalo J, Pelkonen O. (2009) Functional expression, inhibition and induction of CYP enzymes in HepaRG cells. *Toxicol Vitro* **23**:748-753.

Yong WP, Wang LZ, Tham LS, Wong CI, Lee SC, Soo R, Sukri N, Lee HS, and Goh BC. (2008) A phase I study of docetaxel with ketoconazole modulation in patients with advanced cancers. *Cancer Chemother Pharmacol* **62**:243-251.

Yu KS, Cho JY, Jang IJ, Hong KS, Chung JY, Kim JR, Lim HS, Oh DS, Yi SY, Liu KH, Shin JG, Shin SG. (2004) Effect of the CYP3A5 genotype on the pharmacokinetics of intravenous midazolam during inhibited and induced metabolic states. *Clin Pharmacol Ther* **76**:104-112.

Zeilinger K, Holland G, Sauer IM, Efimova E, Kardassis D, Obermayer N, Liu M, Neuhaus P, Gerlach JC. (2004) Time course of primary liver cell reorganization in three-dimensional high-density bioreactors for extracorporeal liver support: An immunohistochemical and ultrastructural study. *Tissue Eng* **10**:1113-1124.

Zeilinger K, Sauer IM, Pless G, Strobel C, Rudzitis J, Wang A, Nussler AK, Grebe A, Mao L, Auth SH, Unger J, Neuhaus P, Gerlach JC. (2002) Three-dimensional co-culture of primary human liver cells in bioreactors for in vitro drug studies: Effects of the initial cell quality on the long-term maintenance of hepatocyte-specific functions. *Altern Lab Anim* **30**:525-538.

Zeilinger K, Schreiter T, Darnell M, Soderdahl T, Lubberstedt M, Dillner B, Knobeloch D, Nussler AK, Gerlach JC, and Andersson TB. (2011) Scaling Down of a Clinical Three-Dimensional Perfusion Multicompartment Hollow Fiber Liver Bioreactor Developed for Extracorporeal Liver Support to an Analytical Scale Device Useful for Hepatic Pharmacological In Vitro Studies. *Tissue Eng Part C Methods* Epub 2011

Footnotes

Part of this work was presented at the ISSX meeting, 2009 May 17-20, Lisbon, Portugal and the AAPS meeting, 2009 November 8-12, Los Angeles, CA. Abstract title: “Cytochrome P450 induction in HepaRG cells cultured in a dynamic 3D bioreactor”

Requests to receive reprints should be sent to

Tommy B. Andersson

DMPK Centre of excellence

AstraZeneca R&D Mölndal

S-431 83 Mölndal

Sweden

E-mail: tommy.b.andersson@astrazeneca.com

Legends for figures

Fig. 1. Multi-compartment perfusion bioreactor with a volume of 2 mL used for 3D culture of HepaRG cells. A) Arrangement of capillaries in the bioreactor; two independently perfused capillary systems (red and blue) serve for culture medium perfusion of the cells located in the extra-capillary space (cell compartment), the third capillary system (yellow) serves for oxygen/CO₂ exchange. B) Bioreactor with connections for medium perfusion, gas supply and cell inoculation into the cell compartment. C) Bioreactor perfusion system with tubing for medium recirculation, feeding and outflow. The recirculation pump controls the speed of medium perfusion through the bioreactor and the feed pump supplies the system with fresh medium from the medium bottle. The sampling port enables substance injection and sampling. The cells in the bioreactor are continuously supplied with air and CO₂.

Fig. 2. Time course of the proliferation, differentiation and experimental phases in HepaRG cells cultured in bioreactors (n=3). Time intervals between different treatments of the cells are indicated between the arrows. The first CYP activity experiment (CYP activity 1) was performed 3 days after DMSO removal. CYP activities were assessed by adding marker substrates to the bioreactor medium and measuring metabolite formation in the perfusate over 6 h. The recirculating medium was washed out after each CYP activity experiment. The effects of ketoconazole and rifampicin on CYP dependent activities were sequentially investigated. The last CYP activity experiment (CYP activity 6) was performed 2-17 days after assessing the effect of rifampicin treatment on the CYP activities (CYP activity 5).

Fig. 3. Immunohistochemical (IHC) staining (brown colour) of apical efflux transporters P-gp (A), MRP2 (B) and the metabolic enzyme CYP3A4 (C) in HepaRG bioreactor tissue using monoclonal antibodies. Both P-gp and MRP2 are located to one side of the hepatocyte-like

cells showing bile canaliculi-like structures. The distribution of the HepaRG cells between two capillaries is shown in A.

Fig. 4. Left: Immunofluorescence (IF) staining of the biliary canaliculi cell marker CK19 (green) in HepaRG bioreactor tissue using monoclonal antibodies. Nuclei are counterstained with DAPI (blue). Right: The corresponding phase contrast image.

Fig. 5. The average daily production of lactate and albumin and release of LDH and AST in HepaRG bioreactors during the proliferation (white bar), differentiation (black bar) and experimental (patterned bar) phases. Lactate and albumin production (A) and LDH and AST release (B) are shown. The bars represent the mean values \pm SD of the average daily production or release in HepaRG bioreactors (n=3). The levels of significance of changes between the differentiation and experimental phases, respectively, compared to the proliferation phase are provided in the figure, * $p < 0.05$, ** $p < 0.01$, and *** $p < 0.001$.

Fig. 6. Comparison of CYP specific activities in bioreactors housing differentiated HepaRG cells 3 days after DMSO removal (solid line) and 2-4 weeks later (dotted line), which are CYP activity 1 and 6, respectively, according to Figure 2. The CYP cocktail was added to the bioreactor recirculation at $t=0$ h. The graphs show the concentration time profiles over 6 h and the formation rates of the formed metabolites in HepaRG cells cultured in the bioreactor: (A) paracetamol (CYP1A1/2 activity), (B) 4-hydroxydiclofenac (CYP2C9 activity), (C) 1'-hydroxymidazolam (CYP3A4 activity) and (D) hydroxybupropion (CYP2B6 activity). Results are given as means \pm S.D. (n=3 bioreactors).

DMD # 37721

Fig. 7. The midazolam 1'-hydroxylase (CYP3A4) activity in bioreactor cultured HepaRG cells before (solid line) and during (dotted line) ketoconazole treatment, which are CYP activity 2 and 3, respectively, according to Fig 2. Results are given as means \pm S.D., (n= 3 bioreactors).

Fig. 8. The midazolam 1'-hydroxylase (CYP3A4) activity (A) and bupropion hydroxylase (CYP2B6) activity (B) in bioreactor cultured HepaRG cells before (solid line) and directly after (dotted line) rifampicin treatment, which are CYP activity 4 and 5, respectively, according to Fig. 2. Results are given as means \pm S.D. (n=3 bioreactors).

Tables

Table 1. The effect of ketoconazole on the 1'-hydroxymidazolam (CYP3A4) pharmacokinetics in HepaRG cells cultured in the bioreactor. The 1'-hydroxymidazolam pharmacokinetics in cells during ketoconazole exposure (CYP activity 3 in Fig. 2) are compared with the pharmacokinetics directly before (CYP activity 2 in Fig. 2) introducing ketoconazole into the system. The results are obtained from three different bioreactors. Published results on the effect of ketoconazole *in vivo* on midazolam pharmacokinetics are also presented in the Table.

	Without Ketoconazole	With ketoconazole	Change
HepaRG bioreactor			
Formation rate 1'-hydroxymidazolam (nmol/h)	1.3 ± 0.45	0.41 ± 0.13 *	-69 ± 2.9 %
<i>In vivo</i> (Tham et al., 2006)			
CL _{midazolam} (L/h)	26 ± 12	4.5 ± 1.8	-83 %

*HepaRG bioreactor: Mean ± S.D., n=3, *p ≤ 0.05, **p < 0.01, and ***p < 0.001*

Table 2. The effect of rifampicin on 1'-hydroxymidazolam (CYP3A4) (A) and hydroxybupropion (CYP2B6) (B) pharmacokinetics in HepaRG cells cultured in the bioreactor. The 1'-hydroxymidazolam and hydroxybupropion pharmacokinetics in cells treated with rifampicin (CYP activity 5 in Fig. 2) are compared with the pharmacokinetics directly before (CYP activity 4 in Fig. 2) introducing rifampicin into the system. The results are obtained from three different bioreactors.

Published results on the effect of rifampicin *in vivo* on midazolam and hydroxybupropion pharmacokinetics are also presented in the Table.

A

	Before rifampicin treatment	After rifampicin treatment	Fold change
HepaRG bioreactor			
Formation rate _{1'-hydroxymidazolam} (nmol/h)	0.93 ± 0.25	4.4 ± 2.2 *	5.5 ± 4.0
<i>In vivo</i> (Yu et al., 2004)			
CL _{midazolam} (L/h*70 kg)	33 ± 10	62 ± 36	1.9

B

	Before rifampicin treatment	After rifampicin treatment	Fold change
HepaRG bioreactor			
Formation rate _{Hydroxybupropion} (nmol/h)	0.062 ± 0.017	0.38 ± 0.085 **	6.3 ± 1.5
<i>In vivo</i> (Kharasch et al, 2008)			
Formation CL _{Hydroxybupropion} (mL/min)	62 ± 47	249 ± 189	3.8

*HepaRG bioreactor: Mean ± S.D., n=3, *p ≤ 0.05, **p < 0.01, and ***p < 0.001*

Figure 1

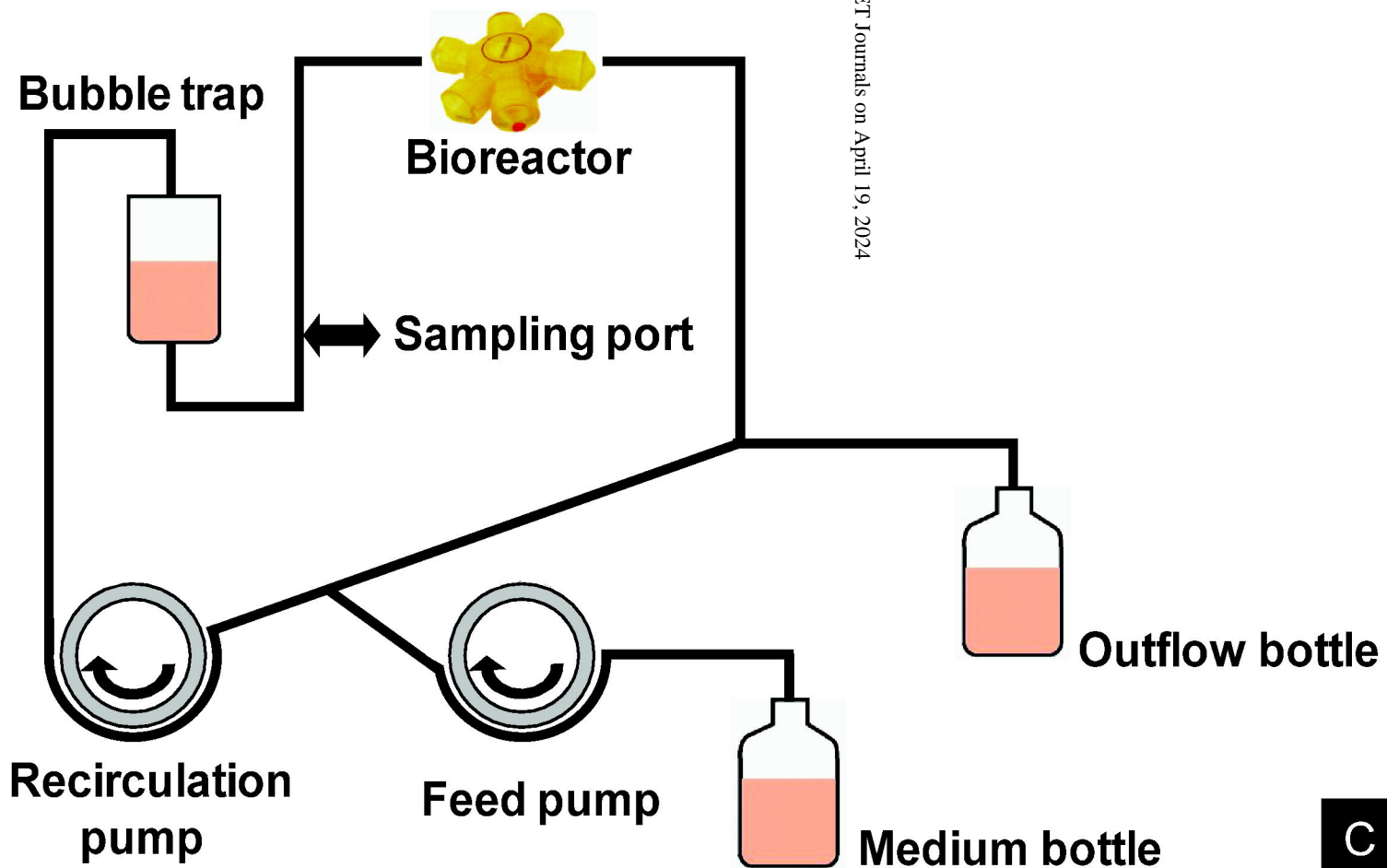
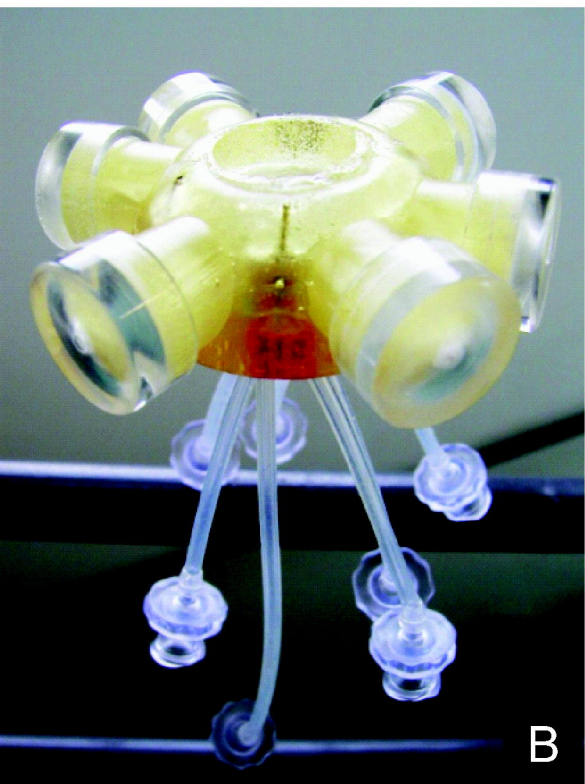
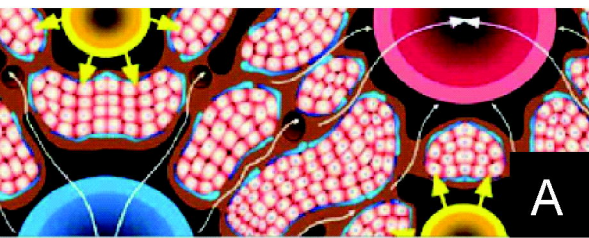


Figure 2

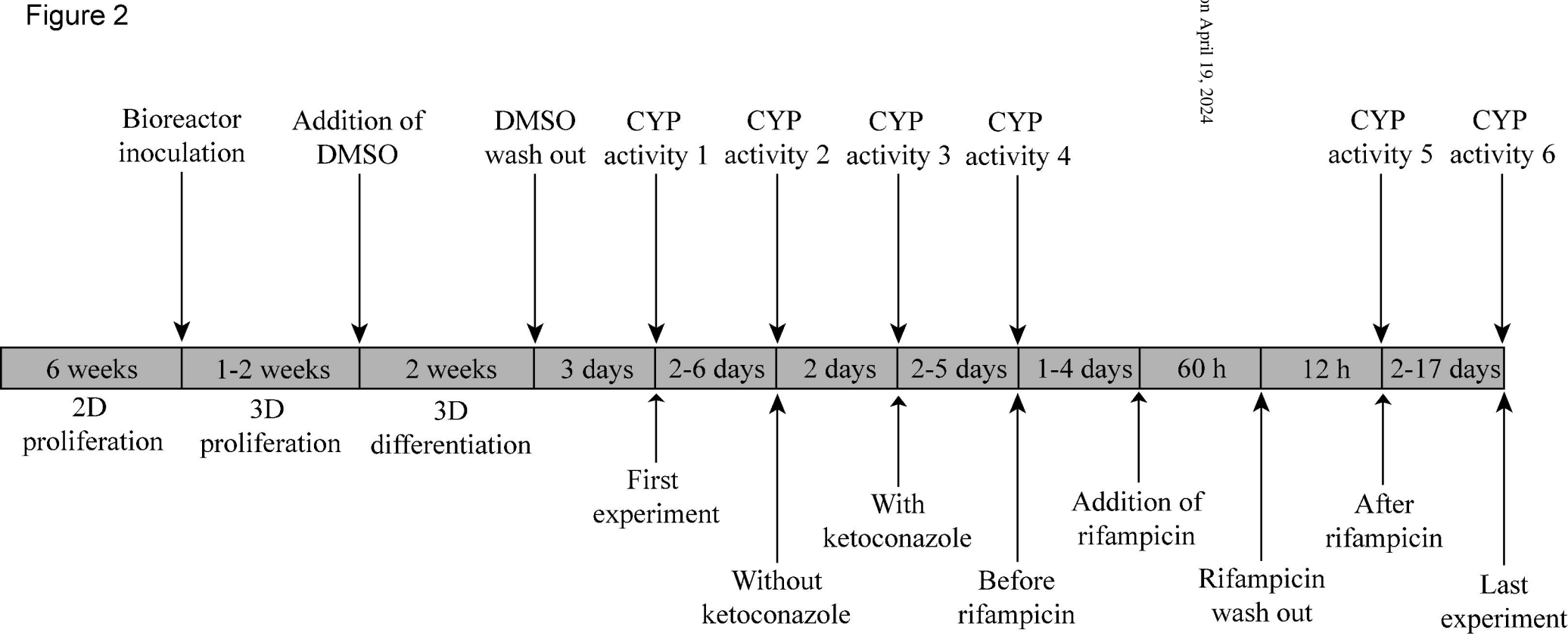


Figure 3

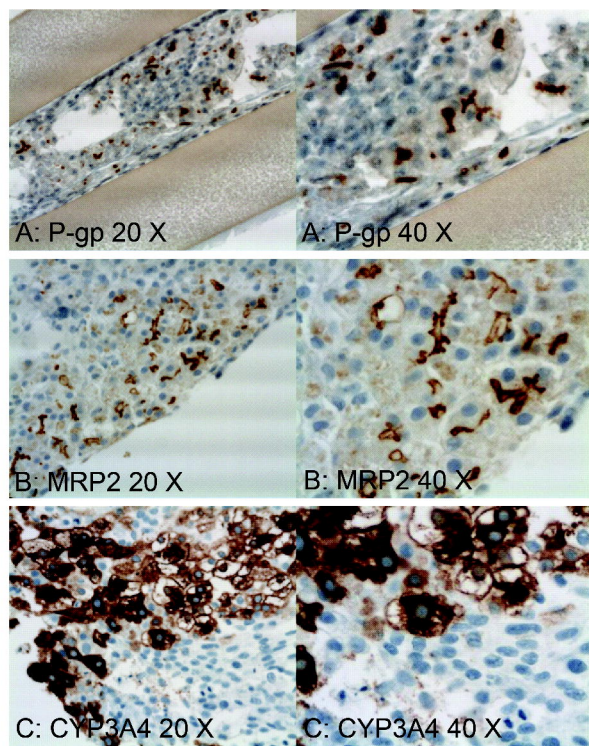


Figure 4

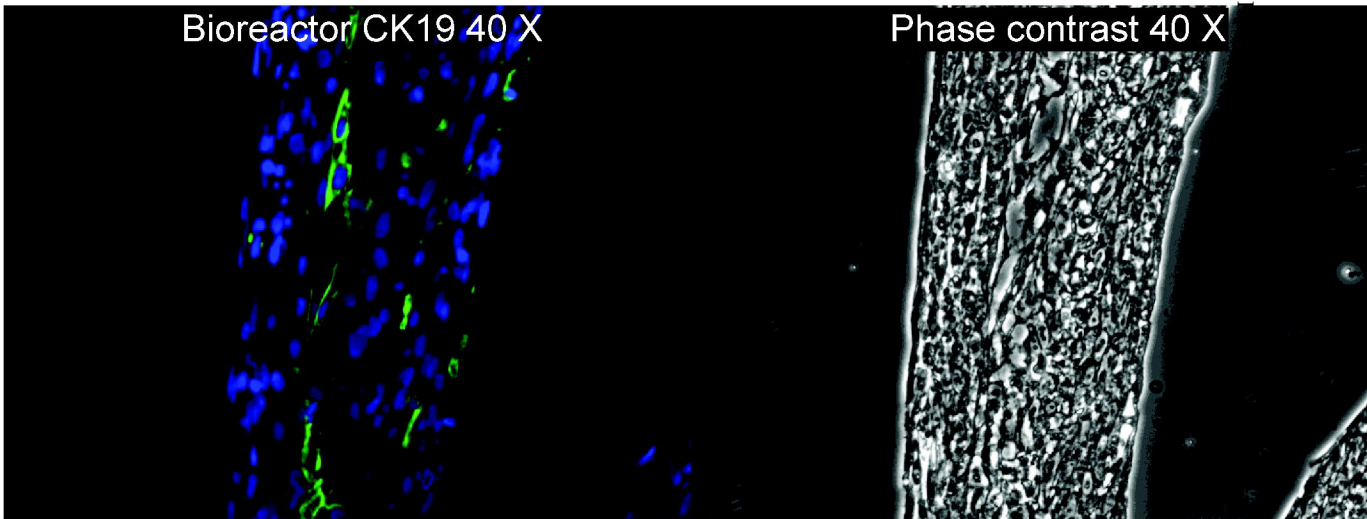


Figure 5

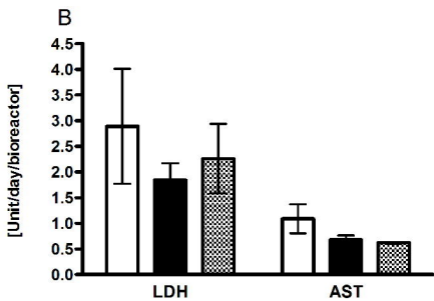
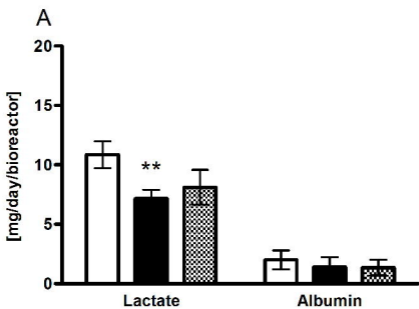


Figure 6

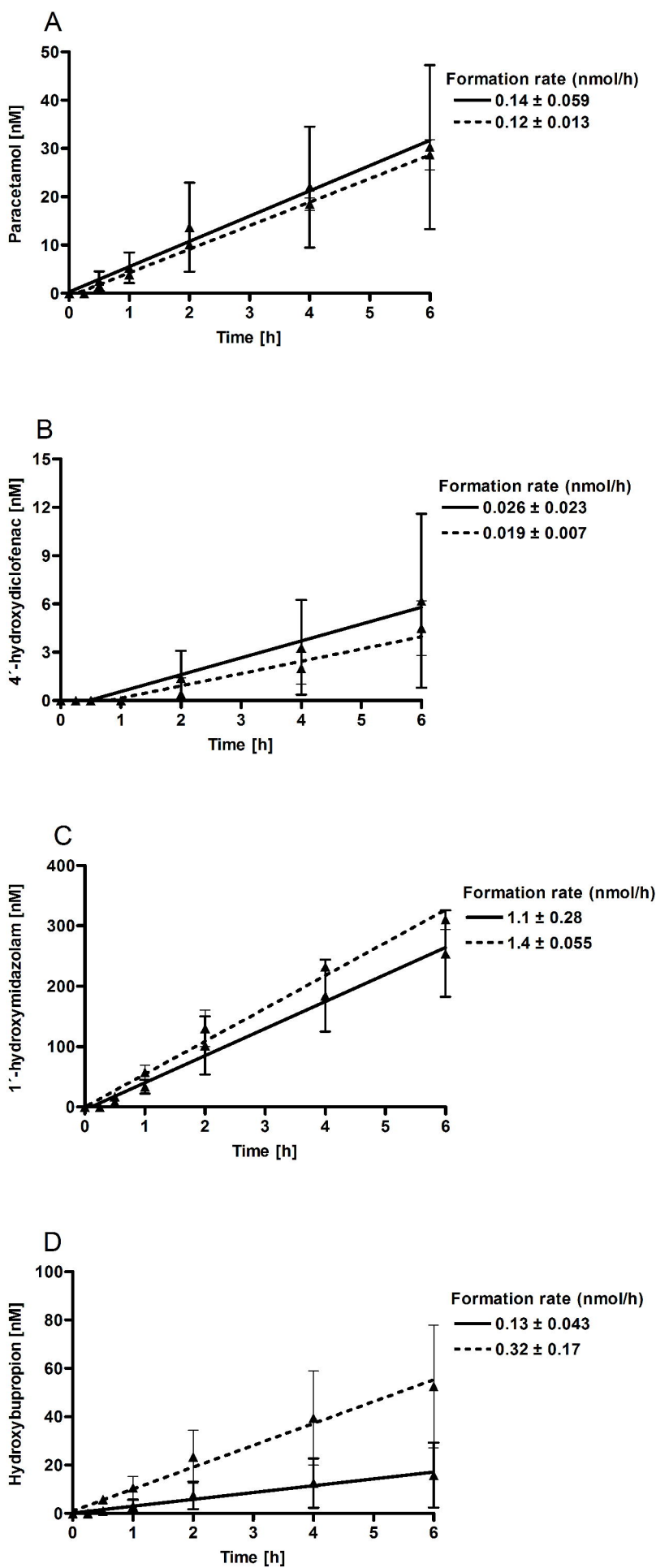


Figure 7

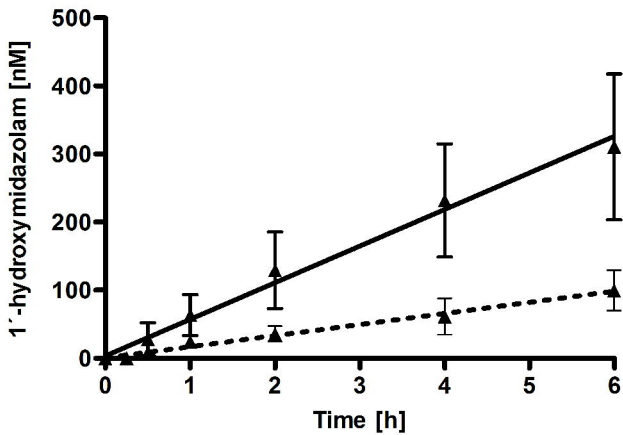


Figure 8

